

Ferroelectricity in the Magnetic E-Phase of Orthorhombic Perovskites

Ivan A. Sergiyenko,^{1,2} Cengiz Sen,³ and Elbio Dagotto^{1,2}¹Materials Science and Technology Division, Oak Ridge National Laboratory, Oak Ridge, TN 37831, USA²Department of Physics & Astronomy, The University of Tennessee, Knoxville, TN 37996, USA³National High Magnetic Field Laboratory and Department of Physics, Florida State University, Tallahassee, FL 32310, USA

We show that the symmetry of the spin zigzag chain E phase of the orthorhombic perovskite manganites and nickelates allows for the existence of a finite ferroelectric polarization. The proposed microscopic mechanism is independent of spin-orbit coupling. We predict that the polarization induced by the E-type magnetic order can potentially be enhanced by up to two orders of magnitude with respect to that in the spiral magnetic phases of $TbMnO_3$ and similar multiferroic compounds.

PACS numbers: 75.80.+q, 75.50.Ee, 77.80.-e, 75.47.Lx

Introduction. The switching of the electric polarization P by a magnetic field of a few Tesla discovered in $TbMnO_3$ [1] and $TbMn_2O_5$ [2] has ignited enormous interest in a class of materials that can be termed improper magnetic ferroelectrics (IMF's). While there is no intrinsic ferroelectric (FE) instability in the IMF's, P emerges due to its coupling to the primary magnetic order parameter. Hence, the FE phase transition coincides with the corresponding magnetic transition, and P is very sensitive to magnetic field induced changes of the magnetic state [1, 2, 3, 4, 5, 6, 7, 8, 9]. Symmetry imposes rather strict conditions on the possible magnetic order parameters: the magnetic structure must have low enough symmetry in order for the system to form a polar axis. As a consequence, the IMF's often have complicated noncollinear structures, including spiral and incommensurate [6, 7, 8, 9, 10, 11, 12, 13], while the IMF phases with collinear magnetism are rare [14, 15]. Noncollinear magnetic structures are stabilized due to either competing interactions (frustration) or anisotropies generated by spin-orbit coupling, which leads to reduced transition temperatures and weaker order parameters. The magnitude of P (~ 0.1 C/cm²) is also affected by its weak coupling to magnetism. In turn, collinear IMF's may prove more promising for future applications as they are less prone to the obstacles mentioned above.

In our present study we turn our attention to the collinear E-type magnetic phase that has been observed in perovskite manganites [16, 17] and nickelates [18, 19, 20, 21]. First, we show that this is a previously overlooked example of an IMF. Second, in contrast to the most extensively theoretically studied case of spiral magnetism [22, 23, 24], the mechanism responsible for ferroelectricity in the magnetically ordered phase does not rely on the presence of an anisotropic Dzyaloshinskii-Moriya interaction. In our case, P appears due to a gain in the band energy of the e_g electrons in the double-exchange model. We estimate that P can be potentially larger than that in the spiral magnets by up to two orders of magnitude, thus paving a way for IMF's to reach the values of P common for other multiferroic systems with better

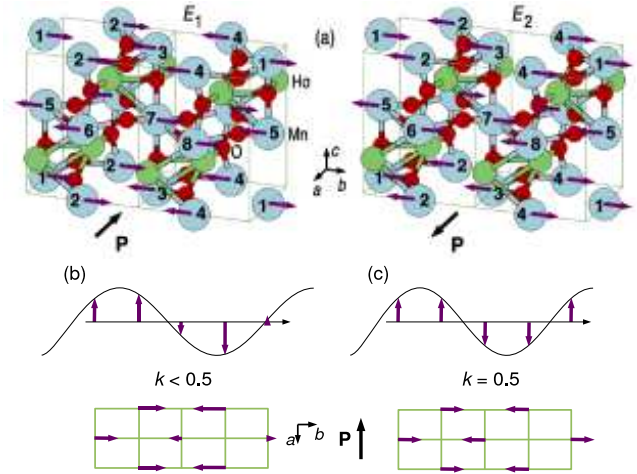


FIG. 1: (Color online) (a) Magnetic unit cells of the two E-phase domains in $HoMnO_3$ corresponding to the $(E_1; 0; P_a)$ and $(0; E_2; P_a)$ solutions of (2). The arrows on the Mn atoms denote the directions of their spins. The FE displacements are not shown, but the direction of P is indicated. (b) The simple sine-wave magnetic structure of $HoMnO_3$ for $T_L < T < T_N = 42 \div 47.5$ K [16]. (c) The E-phase magnetic structure below T_L .

ferroelectric properties [25, 26].

In the perovskite manganite family $RMnO_3$ (space group $Pbnm$), the E-phase was first reported for $R = Ho$ as a result of magnetic structure refinement by neutron diffraction [16]. The magnetic unit cell of the E-phase, forming at low temperature below $T_L = 26 \div 29.6$ K [16, 27], is shown in Fig. 1 (a). The Mn atoms with parallel spins form zigzag chains in the ab -plane, with the chain link equal to the nearest-neighbor Mn-Mn distance. The neighboring zigzag chains in the b -direction have antiparallel spins. Figures 1 (b) and (c) show that the equal-spin E-phase structure can be obtained from the simple sine-wave structure by locking-in its modulation vector $k_b = \frac{1}{2}$ and re-tuning its phase. The ab -planes are stacked antiferromagnetically (+ -) along the c -direction. Interestingly, Lorenz et al. [27] reported on a

large magnetic field dependence of the dielectric constant below T_L , which may be an indication of the multiferroic state.

Landau theory. Independently of the microscopic mechanism, the possibility of a FE state in magnets can be examined by considering the symmetry allowed terms in the Landau potential [6, 11, 24, 28, 29]. We define the symmetric coordinates corresponding to the E-phase as

$$\begin{aligned} E_1 &= S_1 + S_2 - S_3 - S_4 - S_5 - S_6 + S_7 + S_8; \\ E_2 &= S_1 - S_2 - S_3 + S_4 - S_5 + S_6 + S_7 - S_8; \end{aligned} \quad (1)$$

where S_i is the spin of the i th Mn atom in the magnetic unit cell, as shown in Fig 1(a). Since the Mn spins in HoMnO_3 point along the b -axis [16], below we consider only the b -components of $E_{1,2}$ denoted by $E_{1,2}$. However, the expression for the Landau potential derived below is valid for any component of $E_{1,2}$. E_1 and E_2 span an irreducible representation of the space group $P6mm$ corresponding to $k = (0\frac{1}{2}0)$. The properties of this representation are summarized in Table I. Taking into account that P transforms as a polar vector, we obtain the following form of the Landau potential corresponding to the E-phase,

$$\begin{aligned} F &= a(E_1^2 + E_2^2) + b_1(E_1^2 + E_2^2)^2 + b_2E_1^2E_2^2 \\ &+ c(E_1^2 - E_2^2)P_a + d(E_1^2 - E_2^2)E_1E_2P_b + \frac{1}{2}P^2; \end{aligned} \quad (2)$$

where χ is the dielectric susceptibility of the paraelectric phase, and the other coefficients are phenomenological parameters. Minimizing F with respect to P , we obtain $P_a = -c(E_1^2 - E_2^2)$; $P_b = d(E_1^2 - E_2^2)E_1E_2$, and $P_c = 0$. Therefore, each of the four domains of the E-phase [(E_1);0] and (0; E_2)] is IMF with the polarization along the a -axis and different signs of P_a for E_1 and E_2 . We also notice that the b -axis component of P can be locally present within the domain walls where E_1 and E_2 coexist [30].

The E-type phase in the nickelates also consists of spin zigzag chains that have a different direction in the ab -plane and a different stacking along the c -axis (+ + ...) [18, 19, 20, 21]. The corresponding modulation vector is $k = (\frac{1}{2}0\frac{1}{2})$. The Landau theory analysis leads to results similar to the manganite case. For nickelates, the symmetric coordinates E_1 and E_2 (not given here) are written in terms of 16 Ni spins of the magnetic unit cell which is 4 times the crystallographic unit cell. It leads to a Landau potential similar to (2) with P_a replaced by P_b in the fourth term and $d = 0$. Thus, P in the E-phase of nickelates is parallel to the b -axis.

Microscopic model. To understand microscopically the possible mechanism of ferroelectricity in the E-phase we use Monte Carlo (MC) simulations to study the ground state properties of the following Hamiltonian formanganites based on the orbitally degenerate double-exchange

TABLE I: Matrices of the generators of space group $P6mm$ in the irreducible representation spanned by E_1, E_2 . The space group elements are denoted (rjkL), where r is the identity operation 1, two-fold rotation $2_{a;c}$, inversion I , or time reversal 1^0 followed by the translation $\mathbf{t} = ha + kb + lc$.

	$(2_{a;c} \frac{1}{2}0)$	$(2_{c;0} \frac{1}{2})$, $(I 00)$	$(1 010)$, $(1^0 000)$
E_1	1 0	0 1	1 0
E_2	0 1	1 0	0 1

model [31, 32, 33] with one e_g -electron per Mn^{3+} ion,

$$\begin{aligned} H &= \sum_{i,j} X_{ij} C_{i;j+a} t_{ia}^{\uparrow\downarrow} d_{i+a}^{\uparrow\downarrow} + J_{AF} \sum_i S_i \cdot \mathbf{S}_{i+a} \quad (3) \\ &+ \sum_i X_{ia} \left(Q_{1i} \hat{p}_i + Q_{2i} \hat{x}_i + Q_{3i} \hat{z}_i \right) + \frac{1}{2} \sum_{im} X_{im} Q_{mi}^2; \end{aligned}$$

where $d_i^{\uparrow\downarrow}$ is the creation operator for the e_g electron on orbital $\mathbf{d} = x^2 - y^2$ (a); $3z^2 - r^2$ (b); $a = x; y$ is the direction of the link connecting the two nearest neighbor Mn sites; and S_i is the classical unit spin, given by the polar angle θ_i and azimuthal angle ϕ_i , representing the electrons occupying the t_{2g} orbitals on the i -th Mn site. The t_{2g} spins interact directly through the antiferromagnetic superexchange $J_{AF} > 0$. $C_{i;j} = \cos\frac{\phi_i}{2} \cos\frac{\phi_j}{2} + \sin\frac{\phi_i}{2} \sin\frac{\phi_j}{2} e^{i(\phi_i - \phi_j)}$ is the double-exchange factor arising due to the large Hund's coupling that projects out the e_g electrons with spin antiparallel to S_i . Q_{mi} represent the classical adiabatic phonon modes, with stiffnesses ω_m , due to the displacements of the ligand oxygen ions surrounding the i -th Mn site. The phonon stiffnesses were chosen as follows { for the Jahn-Teller modes: $\omega_1 = 2:0$, $\omega_2 = \omega_3 = 1:0$; for the FE mode $\omega_{FE} = 8:0$ and for the rest of the modes, $\omega = 10:0$. Except for the Jahn-Teller modes [31, 32], this choice is driven only by the efficiency of the MC simulations, and it does not reflect the actual frequencies of the phonon modes, which are presently unknown. We illustrate below how P can be obtained in physical units. The third term in Eq. (3) is the Jahn-Teller coupling with constant χ and the e_g -orbital operators $\hat{p}_i = d_{ia}^{\uparrow} d_{ia}^{\downarrow} + d_{ib}^{\uparrow} d_{ib}^{\downarrow}$, $\hat{x}_i = d_{ia}^{\uparrow} d_{ib}^{\downarrow} + d_{ib}^{\uparrow} d_{ia}^{\downarrow}$ and $\hat{z}_i = d_{ia}^{\uparrow} d_{ia}^{\downarrow} - d_{ib}^{\uparrow} d_{ib}^{\downarrow}$.

Our improvements over previous approaches to this model are the following. First, we explicitly consider the dependence of the hopping parameters $t_{ia}^{\uparrow\downarrow}$ on the angle of the Mn-O-Mn bond θ'_{ia} . Taking into account only the largest Mn-O bond contribution, we find [34] $t_{aa}^x = t_{aa}^y = t \cos^3 \theta'$, $t_{bb}^x = t_{bb}^y = t \cos \theta' = 3$, $t_{ab}^x = t_{ba}^x = t_{ab}^y = t_{ba}^y = t \cos^2 \theta' = 3$, where $t = \frac{3}{4} (pd)^2$ is taken as the energy unit hereafter. We neglect the θ' dependence of J_{AF} since it has a smaller energy scale than t . Second, Q_{mi} 's are defined such that the elastic energy term in (3) is minimal for $\theta'_{ia} = \theta'_{i0} < 180^\circ$. This allows us to model the initial structural buckling (GdFeO₃-type)

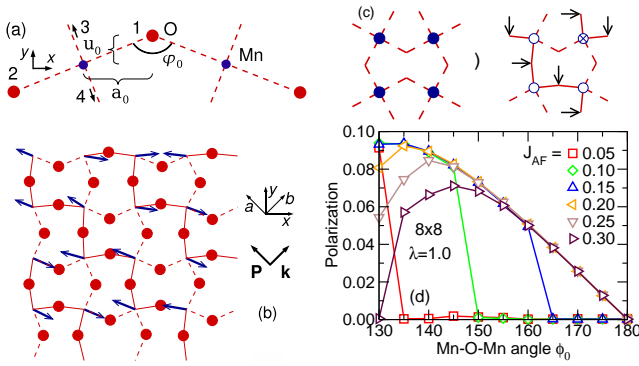


FIG. 2: (Color online) (a) The starting con guration of a Mn-O-Mn bond. Numbers 1-4 enumerate the O atoms surrounding one Mn. (b) A MC snapshot of the IMF E-phase at $T = 0.01$. The ferromagnetic zigzag chain links are shown as solid lines. The displacements of the oxygen atoms are exaggerated. (c) Left. The local arrangement of the Mn-O bonds with disordered Mn spins (full circles). Right. Oxygen displacements (arrows) within the chains of opposite Mn spins (open and crossed circles) in the E-phase (see also Refs.[3, 15]). (d) MC results for the polarization at $T = 0.01$ for different values of J_{AF} .

distortion present in the orthorhombic perovskites [35]. In particular, the buckling mode is defined in two dimensions as $Q_{buckley,i} = Y_{i1} - Y_{i2} - x_{i3} + x_{i4} - (1)^{i_x + i_y} 4u_0$; where x_{ik}, y_{ik} are the displacements of the oxygen atoms from their ideal position in the 180 Mn-O-Mn bond, $u_0 = a_0 \cot \frac{\phi_0}{2}$, and a_0 is the Mn-O distance in the 180 Mn-O-Mn bond [see Fig.2 (a)]. Since the buckling distortion in the considered perovskites is present at temperatures well above the magnetic transitions, we consider ϕ_0 as a fixed parameter of the model. For HoMnO_3 , ϕ_0 is close to 144 [35]. As shown below, this distortion plays a crucial role in generating ferroelectricity in the E-phase. Introducing $\phi_0 < 180$ effectively reduces the symmetry of the Hamiltonian (3), although it is still invariant with respect to the inversion symmetry centers located at the every Mn site. The FE polarization emerges only due to the spontaneous symmetry breaking caused by the E-phase magnetic order.

Monte Carlo results. Many results of the model (3) regarding magnetic and orbital order, without the modifications mentioned above, are reported in Ref. [32]. Our present treatment essentially confirms those results. The ground state phase diagram in two dimensions contains the ferromagnetic phase, E-phase, and the Neel-like G-phase. Here we focus our attention on the new results directly related to the ferroelectricity of the E-phase. A typical low-temperature E-phase MC snapshot is shown in Fig.2 (b). In accordance with the absence of spin-orbit interaction in Hamiltonian (3), it is invariant with respect to collective spin rotations, therefore the preferred spin direction is chosen randomly in our MC simulations. However, the ferromagnetic zigzag chains are clearly es-

tablished in the ground state. As is seen from the snapshot, the double-exchange physics plays a crucial role in the formation of the FE state. Due to the factor C_{ij+} the electron hopping is prohibited between Mn atoms with opposite t_{2g} spins. Hence, the displacement of the corresponding oxygen atom perpendicular to the Mn-Mn bond (these displacements are not Jahn-Teller active) is only due to the elastic energy, which favors the bond angle ϕ_0 . On the contrary, hopping is allowed along the ferromagnetic zigzag chains [36]. Since hopping energy is minimal for the 180 bond, the competition between the hopping and elastic energies generally results in a bond angle ϕ_0 , such that $\phi_0 < \phi < 180$ [see Fig.2 (c)]. Since ϕ only depends on the nature of the bond (ferromagnetic vs. antiferromagnetic), the direction of the oxygen displacements is the same in all zigzag chains, even though neighboring chains have opposite spin. This leads to the overall coherent displacement of the center of mass of the O atoms with respect to the Mn sublattice, similarly as proposed in Ref. [15] for the field-induced phase of TbMnO_3 . It is easy to see from Fig.2 (b, c) that the resulting FE polarization points along the diagonal connecting the next-nearest-neighbor Mn atoms, i.e. the a-axis in the orthorhombic setting, in perfect agreement with Landau theory.

The value of P. Figure 2 (d) shows the calculated absolute value of the polarization P_{calc} , defined as the oxygen displacement per one "unit cell" containing one Mn and two O atoms averaged over MC steps, plotted versus ϕ_0 for different values of J_{AF} . P vanishes for $\phi_0 = 180$ for all values of J_{AF} . In this case both the hopping and elastic energies are optimal when $\phi = \phi_0 = 180$, the same for ferromagnetic and antiferromagnetic bonds. To demonstrate that this is also consistent with the symmetry arguments of Landau theory, we note that the symmetry of the lattice with 180 bonds is higher than that with $\phi_0 < 180$. Particularly, additional inversion centers are located at the O sites if $\phi_0 = 180$. While the E-type magnetic structure breaks inversion symmetry for centers located at the Mn sites, it is invariant with respect to the O-site centers, and thus the magnetic phase transition cannot induce FE order. In terms of the Landau potential (2), the coefficients c and d must be zero in this case.

The MC calculated value of the polarization P_{calc} for $\phi_0 = 145$ corresponding to HoMnO_3 reaches 0.08. It can be shown from the model (3), that the FE displacements scale as $t_{FE} a_0$. In the simulations we set $t = 1$ and $a_0 = 1$, and the polarization in the physical units, in the point charge approximation, is given by $P = \frac{12 e t_{FE}}{F_E a_0 V_0} P_{\text{calc}}$; where e is the elementary charge, V_0 is the FE phonon stiffnesses in the physical units, and V_0 is the unit cell volume. Using $a_0 = 2.35 \text{ \AA}$, $V_0 = 226 \text{ \AA}^3$ [16], $t = 0.1 - 0.5 \text{ eV}$ [31], $V_0 = 1.5 \text{ eV/\AA}^2$ [23], we obtain a range of values for P between 0.5 and 12

C/cm^2 , substantially larger than the P observed in helical IMFs. We can also estimate P from the known experimental results for TbMnO_3 . Its crystal structure is modulated in the collinear sine-wave phase with wave vector $k_L = 2k_M$ where $k_M = 0.29$ is the magnetic wave vector. The displacement of the O atom in a Mn-O chain running along the x- or y-direction [see Fig. 2 (b)] is given by $r_n = r_0 (1)^n \text{fcos } k_M + \cos[(2n+1)k_M + 2]g$, for the magnetic structure defined by $S_a = S_c = 0$, $S_b = S_b^0 \cos(nk_M + \phi)$ [23]. If $k_M \in [1=2, 2]$, then $r_n^a = r_n^b = 0$ and the state is paraelectric. The E-phase corresponds to $k_M = 1=2, 3=4$, and hence $r_n^a = r_n^b$ represents a coherent displacement within one chain. While the b and c components of r_0 have different signs in different chains, r_0^a 's are the same. Considering the TbMnO_3 value $r_0 = 10^{-2}$ Å [37] as an estimate for r_0^a in HoMnO_3 , we obtain $P \approx 2 C/\text{cm}^2$ consistent with the calculated values.

Summary. We argue that the symmetry of the spin zigzag chain magnetic E-phase in orthorhombic perovskites with buckling distortion of the oxygen octahedra allows the formation of a polar axis along the a-axis. The microscopic mechanism of ferroelectricity is independent of spin-orbit coupling, and P can potentially be up to two orders of magnitude higher than that in the helical IMFs. Note that the ideas described here are general, and the E-phase provides just one example. In fact, the mechanism is similar to the recently proposed explanation for the ferroelectricity found in TbMnO_3 at high fields [15], and our effort provides a theoretical basis for that interesting scenario. As to the E-phase nickelates, the microscopic model considered here is not applied to them directly [38]. However, we expect that the same interplay between the optimization of the electron hopping and the elastic energy in the presence of the buckling distortion will lead to ferroelectricity.

We thank M. Angst, D. Argyriou, T. Egami, D. Mandrus, and D. Singh for inspiring discussions, as well as T. Kimura and B. Lorenz for providing us with their unpublished results. Research at ORNL is sponsored by the Division of Materials Sciences and Engineering, Office of Basic Energy Sciences, U.S. Department of Energy, under contract DE-AC05-00OR22725 with ORNL, managed and operated by UT-Battelle, LLC. This work is also supported in part by NSF DMR-0443144 and NSF DMR-0072998. We have used the SPFF software developed at ORNL (<http://scicom.pforge.org/spff>).

Note added. Following our prediction, B. Lorenz et al. [39] reported on experimental evidence of ferroelectricity in perovskite HoMnO_3 and YMnO_3 . For the latter, the E-phase was proposed in Ref. [17].

- [2] N. Hur et al, Nature 429, 392 (2004).
 [3] T. Goto et al, Phys. Rev. Lett. 92, 257201 (2004).
 [4] T. Kimura, G. Lawes, and A. P. Ramirez, Phys. Rev. Lett. 94, 137201 (2005).
 [5] T. Kimura et al, Phys. Rev. B 71, 224425 (2005).
 [6] G. Lawes et al, Phys. Rev. Lett. 95, 087205 (2005).
 [7] L.C. Chapon et al, Phys. Rev. Lett. 96, 097601 (2006).
 [8] T. Kimura, J.C. Lashley, and A. P. Ramirez, Phys. Rev. B 73, 220401(R) (2006).
 [9] Y. Yamasaki et al, Phys. Rev. Lett. 96, 207204 (2006).
 [10] G.R. Blake et al, Phys. Rev. B 71, 214402 (2005).
 [11] M. Kenzelmann, A.B. Harris, S. Jonas, et al, Phys. Rev. Lett. 95, 087206 (2005).
 [12] T. Arima et al, Phys. Rev. Lett. 96, 097202 (2006).
 [13] K. Taniguchi et al, Phys. Rev. Lett. 97, 097203 (2006).
 [14] L.C. Chapon et al, Phys. Rev. Lett. 93, 177402 (2004).
 [15] N. A. Kouane, D.N. Argyriou, J. Stremper, et al, Phys. Rev. B 73, 020102(R) (2006).
 [16] A. Muñoz, M.T. Casais, J.A. Alonso, et al, Inorg. Chem. 40, 1020 (2001).
 [17] J.-S. Zhou and J.B. Goodenough, Phys. Rev. Lett. 96, 247202 (2006).
 [18] J.L. Garcia-Muñoz, J. Rodriguez-Carvajal, and P. Lacorre, Phys. Rev. B 50, 978 (1994).
 [19] J.A. Alonso, J.L. Garcia-Muñoz, M.T. Fernandez-Diaz, et al, Phys. Rev. Lett. 82, 3871 (1999).
 [20] M.T. Fernandez-Diaz, J.A. Alonso, M.J.M. Artinez-Lopez, et al, Phys. Rev. B 64, 144417 (2001).
 [21] J.-S. Zhou, J.B. Goodenough, and B.D. Abrowski, Phys. Rev. Lett. 95, 127204 (2005).
 [22] H. Katsura, N. Nagaosa, and A.V. Balatsky, Phys. Rev. Lett. 95, 057205 (2005).
 [23] I.A. Sergiyenko and E.D. Agotto, Phys. Rev. B 73, 094434 (2006).
 [24] M. Mostovoy, Phys. Rev. Lett. 96, 067601 (2006).
 [25] M. Fiebig, J. Phys. D: Appl. Phys. 38, R123 (2005).
 [26] C. Ederer and N.A. Spaldin, Curr. Opin. Solid State Mater. Sci. 9, 128 (2005).
 [27] B. Lorenz, Y.Q. Wang, Y.Y. Sun, and C.W. Chu, Phys. Rev. B 70, 212412 (2004).
 [28] S. Goshen, D. Mukamel, H. Shaked, and S. Shtrikman, Phys. Rev. B 2, 4679 (1970).
 [29] A.B. Harris, T. Yildirim, A. Aharony, and O. Entin-Wohlman, Phys. Rev. B 73, 184433 (2006).
 [30] Although the E-phase is a special case of the simple sine-wave structure, the continuum theory considered in Ref. [24], which predicts $P = 0$, is not applicable to modulation vectors at the edge of the Brillouin zone.
 [31] E.D. Agotto, T. Hotta, and A. Moreo, Phys. Rep. 344, 1 (2001).
 [32] T. Hotta et al, Phys. Rev. Lett. 90, 247203 (2003).
 [33] D.V. Efremov, J. van den Brink, and D.I. Khomskii, Nature Materials 3, 853 (2004).
 [34] J.C. Slater and G.F. Koster, Phys. Rev. 94, 1498 (1954).
 [35] T. Kimura, S. Ishihara, H. Shintani, et al, Phys. Rev. B 68, 060403(R) (2003).
 [36] Although virtual hopping is allowed along the zigzag chains, the E-phase is a band insulator [32].
 [37] T. Kimura, private communication.
 [38] T. Hotta and E.D. Agotto, Phys. Rev. Lett. 92, 227201 (2004).
 [39] B. Lorenz, Y.Q. Wang, and C.W. Chu, cond-mat/0608195.